Quark Pseudo-Distributions at Short Distances

A. V. Radyushkin

Physics Department, Old Dominion University, Norfolk, VA 23529, USA

Thomas Jefferson National Accelerator Facility, Newport News, VA 23606, USA

Abstract

We perform a one-loop study of the small-z_3^2 behavior of the Ioffe-time distribution (ITD) $\mathcal{M}(\nu, z_3^2)$, the basic function that may be converted into parton pseudo- and quasi-distributions. We calculate the corrections on the operator level, so that our results may be later used for pseudo-distribution amplitudes and generalized parton pseudo-distributions. We separate two sources of the z_3^2-dependence at small z_3^2. One is related to the ultraviolet (UV) singularities generated by the gauge link, and another to short-distance logarithms generating perturbative evolution of parton densities. Our calculation explicitly shows that UV-singular terms vanish for $z_3^2 = 0$. The UV divergences are absent in the ratio $\mathcal{M}(\nu, z_3^2)/\mathcal{M}(0, z_3^2)$ ("reduced" ITD). Still, it has a non-trivial short-distance behavior due to $\ln z_3^2\Lambda^2$ terms generating perturbative evolution of the parton densities. We give an explicit expression, up to constant terms, for the reduced ITD at one loop. It may be used in extraction of PDFs from the lattice QCD simulations. We also use our results to get new insights concerning the structure of parton quasi-distributions at one-loop level.

1. Introduction

The usual parton distribution functions (PDFs) $f(x)$ [1] are often mentioned now as "light-cone PDFs", since they are related to matrix elements $M(z, p)$ of the $\langle p|\phi(0)\phi(z)|p\rangle$ type taken on the light cone $z^2 = 0$. The parton *pseudo-distributions* $\mathcal{P}(x, -z^2)$ [2] generalize PDFs for a situation when z is off the light cone, in particular, when z is spacelike $z^2 < 0$. To obtain them, one should treat $M(z, p)$ as a function $\mathcal{M}(\nu, -z^2)$ of the Ioffe time $(pz) \equiv -\nu$ [3] and z^2. Fourier-transforming $\mathcal{M}(\nu, -z^2)$ with respect to ν gives pseudo-PDFs $\mathcal{P}(x, -z^2)$.

As suggested by X. Ji [4], using purely space-like separations $z = (0, 0, 0, z_3)$ (or, for brevity, $z = z_3$) allows one to study matrix elements $M(z_3, p)$ (and hence, the Ioffe-time distributions [5] $\mathcal{M}(\nu, z_3^2)$) on the lattice. To extract PDFs from such studies, one needs to understand the small-z_3^2 behavior of the pseudo-PDFs $\mathcal{P}(x, z_3^2)$.

In any renormalizable theory, a perturbative calculation of the matrix element $M(z_3, p)$ reveals logarithmic $\ln z_3^2$ singularities resulting in the perturbative evolution of PDFs. Further complications arise in quantum chromodynamics (QCD), where the parton fields are connected by a gauge link $E(0, z; A)$. As emphasized by Polyakov [6], perturbative corrections to gauge links (and loops) result in specific ultraviolet divergences requiring an additional renormalization. Studies of the UV and short-distance properties of the QCD bilocal operators $\bar\psi(0)\gamma^\alpha E(0, z; A)\psi(z)$ were performed in Ref. [7].

An important point is that the effects of perturbative gluonic corrections may be formulated on the operator level, without reference to a particular matrix element in which the operator is inserted. This idea was implemented in much detail by Balitsky and Braun [8] who applied it to studies of the light-cone limit. For this reason, they skipped the discussion of the link-specific UV divergences that disappear when $z^2 = 0$.

In the present paper, we perform a one-loop study of the QCD bilocal operators off the light cone. We pay attention both to the UV-singular link-related contributions and to the UV-finite evolution-related terms singular in the $z_3^2 \to 0$ limit. Technically, our calculations are similar to those performed in our paper [9] within the formalism of virtuality distributions [10]. In some aspects, our calculations also resemble those of Ref. [8].

We start, in Section 2, with a short overview of the basic ideas of our approach formulated in Refs. [11, 2]. In Section 3, we outline the calculation of the one-loop diagrams responsible for the behavior of the ITD $\mathcal{M}(x, z_3^2)$ for small z_3. In Section 4, we show that rather simple expressions for the one-loop ITD may be used for a straightforward calculation of the one-loop quasi-PDFs, providing new insights concerning their structure. Section 5 contains the summary of the paper.

2. PDFs

2.1. Ioffe-time distributions

The basic parton distribution functions (PDFs) introduced by Feynman [1] are extracted from the matrix elements of bilocal operators, generically written as $\langle p|\phi(0)\phi(z)|p\rangle$. We use here scalar notations for the partonic fields because complications related to spin are not central to the very concept of PDFs.

In many situations (especially in extraction of parton distributions from the lattice), it is very useful to treat such a matrix element as a function $\mathcal{M}(\nu, -z^2)$ of two Lorentz invariants, the *Ioffe time* $(pz) \equiv -\nu$ and the interval $-z^2$. Thus, we write

$$\langle p|\phi(0)\phi(z)|p\rangle \equiv M(z, p) = \mathcal{M}(-(pz), -z^2) = \mathcal{M}(\nu, -z^2)\,. \tag{2.1}$$

The function $\mathcal{M}(\nu, -z^2)$ is the *Ioffe-time distribution* [5].

It can be shown [11, 12] that, for all contributing Feynman diagrams, the Fourier transform $\mathcal{P}(x, -z^2)$ of the ITD with respect to ν has the $-1 \le x \le 1$ support, i.e.,

$$\mathcal{M}(\nu, -z^2) = \int_{-1}^{1} dx\, e^{ix\nu}\, \mathcal{P}(x, -z^2)\,. \tag{2.2}$$

Note that writing Eq. (2.2) we do not assume that $z^2 = 0$ or $p^2 = 0$, i.e. this relation gives a covariant definition of x.

2.2. Light-cone PDFs

The expressions for various types of parton distributions, all in terms of the same ITD $\mathcal{M}(-(pz), -z^2)$, may be obtained from special choices of z and p. In particular, taking a light-like z, e.g., that having the light-front minus component z_- only, we parameterize the matrix element through the twist-2 parton distribution $f(x)$

$$\mathcal{M}(-p_+ z_-, 0) = \int_{-1}^{1} dx\, f(x)\, e^{-ixp_+ z_-}\ . \tag{2.3}$$

It has the usual interpretation of probability that the parton carries the fraction x of the target momentum component p_+. The inverse relation is given by

$$f(x) = \frac{1}{2\pi} \int_{-\infty}^{\infty} d\nu\, e^{-ix\nu}\, \mathcal{M}(\nu, 0) = \mathcal{P}(x, 0)\,. \tag{2.4}$$

Since $f(x) = \mathcal{P}(x, 0)$, we can say that the function $\mathcal{P}(x, -z^2)$ generalizes the concept of the usual light-cone parton distribution onto intervals z^2 that are not light-like. The functions $\mathcal{P}(x, -z^2)$ will be referred to as parton *pseudo-distributions* [2].

2.3. Quasi-Distributions

Since one cannot have light-like separations on the lattice, it was proposed [4] to consider equal-time separations $z = (0, 0, 0, z_3)$ [or, for brevity, $z = z_3$]. Then, in the $p = (E, 0_\perp, P)$ frame, one introduces quasi-PDF $Q(y, P)$ through a parametrization

$$\mathcal{M}(Pz_3, z_3^2) = \int_{-\infty}^{\infty} dz_3\, Q(y, P)\ e^{iyPz_3}\ . \tag{2.5}$$

The quasi-PDF describes the distribution of parton's $k_3 = yP$ momentum. Using the inverse relation

$$Q(y, P) = \frac{P}{2\pi} \int_{-\infty}^{\infty} dz_3\, e^{-iyPz_3}\, \mathcal{M}(Pz_3, z_3^2)\,, \tag{2.6}$$

we can express the quasi-PDF $Q(y, P)$ in terms of the pseudo-PDF $\mathcal{P}(x, z_3^2)$ corresponding to the $z = z_3$ separation

$$Q(y, P) = \frac{P}{2\pi} \int_{-1}^{1} dx \int_{-\infty}^{\infty} dz_3\, e^{-i(y-x)Pz_3}\, \mathcal{P}(x, z_3^2)\,. \tag{2.7}$$

Note that when $\mathcal{P}(x, z_3^2)$ does not depend on z_3, i.e., when $\mathcal{P}(x, z_3^2) = f(x)$, the quasi-distribution $Q(y, P)$ does not depend on P, and coincides with the PDF $f(y)$.

It should be noted that the integration variable z_3 in Eq. (2.6) enters into both arguments of the ITD $\mathcal{M}(Pz_3, z_3^2)$. In contrast, the pseudo-PDF $\mathcal{P}(x, z_3^2)$ is obtained through integrating the ITD $\mathcal{M}(\nu, z_3^2)$ just with respect to its first argument,

$$\mathcal{P}(x, z_3^2) = \frac{1}{2\pi} \int_{-\infty}^{\infty} d\nu\, e^{-ix\nu}\, \mathcal{M}(\nu, z_3^2)\,. \tag{2.8}$$

2.4. Transverse momentum dependent distributions

If one treats the target momentum p as longitudinal, $p = (E, \mathbf{0}_\perp, P)$, but chooses z that has a transverse $z_\perp = \{z_1, z_2\}$ component, one can introduce the transverse momentum dependent distributions (TMDs). Namely, taking $z_+ = 0$, one defines the *TMD* $\mathcal{F}(x, k_\perp^2)$ by

$$\mathcal{M}(\nu, z_\perp^2) = \int_{-1}^{1} dx\ e^{ix\nu} \int_{-\infty}^{\infty} d^2\mathbf{k}_\perp e^{i(\mathbf{k}_\perp \mathbf{z}_\perp)} \mathcal{F}(x, k_\perp^2)\,. \tag{2.9}$$

One may also write

$$\mathcal{P}(x, z_\perp^2) = \int d^2\mathbf{k}_\perp e^{i(\mathbf{k}_\perp \mathbf{z}_\perp)} \mathcal{F}(x, k_\perp^2)\,. \tag{2.10}$$

This means that the pseudo-PDF $\mathcal{P}(x, z_\perp^2)$ coincides in this case with the *impact parameter distribution*, a concept that is well known from TMD studies.

While $z = z_3$ corresponds to a purely "longitudinal" separation, the Lorentz invariance requires that $\mathcal{P}(x, -z^2)$ is the same function of $-z^2$ no matter what kind of a space-like z we deal with. In other words, the dependence of $\mathcal{P}(x, z_3^2)$ on its second argument reflects the same physics that leads to TMDs.

2.5. QCD case.

The formulas given above may be used in case of non-singlet parton densities in QCD. The relevant matrix elements are

$$M^\alpha(z, p) \equiv \langle p|\bar\psi(0)\, \gamma^\alpha\, \hat E(0, z; A)\psi(z)|p\rangle\,, \tag{2.11}$$

where $\hat E(0, z; A)$ is the standard $0 \to z$ straight-line gauge link in the quark (fundamental) representation

$$\hat E(0, z; A) \equiv P \exp\left[ig\, z_\nu \int_0^1 dt\, A^\nu(tz)\right]. \tag{2.12}$$

These matrix elements have p^α and z^α parts

$$M^\alpha(z, p) = 2p^\alpha \mathcal{M}_p(-(zp), -z^2) + z^\alpha \mathcal{M}_z(-(zp), -z^2)\,. \tag{2.13}$$

When $z^2 \to 0$, the $\mathcal{M}_p$ part gives the twist-2 distribution, while $\mathcal{M}_z$ is a purely higher-twist contamination. Note, however, that $\mathcal{M}_z$ does not contribute in the standard definition of unpolarized TMDs because it is based on taking $z = (z_-, z_\perp)$ in the $\alpha = +$ component of O^α. Then the z^α-part drops out. As a result, $\mathcal{F}(x, k_\perp^2)$ is related to $\mathcal{M}_p(\nu, z_\perp^2)$ by the scalar formula (2.9).

To keep a simple relation between TMDs and z_3-pseudo-PDFs (and, hence, quasi-PDFs), we need to arrange that the z^α contamination does not contribute to

psedo-PDFs. This is achieved by taking the time component of $M^\alpha(z = z_3, p)$ and defining

$$M^0(z_3, p) = 2p^0 \mathcal{M}_p(\nu, z_3^2) = 2p^0 \int_{-1}^{1} dx \mathcal{P}(x, z_3^2)\, e^{ix\nu} \,. \quad (2.14)$$

The quasi-distribution $Q(y, P)$ is defined in a similar way:

$$M^0(z_3, p) = 2p^0 \int_{-\infty}^{\infty} dy\, Q(y, P)\, e^{iyPz_3} \,. \quad (2.15)$$

As a result, the connection between $Q(y, P)$ and $\mathcal{P}(x, z_3^2)$ is given by the scalar formula (2.7). From now on, we will shorten the notation by using $\mathcal{M}_p \to \mathcal{M}$.

In QCD, $\mathcal{M}(\nu, z_\perp^2)$ contains $\sim \ln z_\perp^2$ terms corresponding to the $\sim 1/k_\perp^2$ hard tail of $\mathcal{F}(x, k_\perp^2)$. Thus, it makes sense to visualize $\mathcal{M}(\nu, z_\perp^2)$ as a sum of a soft part $\mathcal{M}^{\rm soft}(\nu, z_\perp^2)$, that has a finite $z_\perp^2 \to 0$ limit, and a logarithmically singular *hard part* reflecting the evolution. The same applies to $\mathcal{M}(\nu, z_3^2)$.

3. Hard contribution in coordinate space

Even if one starts with a purely soft TMD (or pseudo-PDF), the gluon exchanges generate the hard part. Our goal is to describe this on the operator level, as a modification of the original bilocal operator by gluon corrections.

3.1. Link self-energy contribution

To begin with, we consider the modification resulting from the self-energy correction to the gauge link (see also Refs. [6, 13]). At one loop, it is given by

$$\Gamma_\Sigma(z) = (ig)^2 C_F \frac{1}{2} \int_0^1 dt_1 \int_0^1 dt_2\, z^\mu z^\nu D^c_{\mu\nu}[z(t_2 - t_1)] \,, \quad (3.1)$$

where $D^c_{\mu\nu}[z(t_2 - t_1)]$ is the gluon propagator connecting points $t_1 z$ and $t_2 z$. For massless gluons in Feynman gauge, we have $D^c_{\mu\nu}(z) = -g_{\mu\nu}/4\pi^2 z^2$, and end up with a divergent integral

$$\int_0^1 dt_1 \int_0^1 \frac{dt_2}{(t_2 - t_1)^2} \,. \quad (3.2)$$

This divergence has an ultraviolet origin. For spacelike z, it may be regularized by using the Polyakov prescription [6] $1/z^2 \to 1/(z^2 - a^2)$ for the gluon propagator. Taking $z = z_3$ we have

$$\Gamma_\Sigma(z_3, a) = -\, g^2 C_F \frac{z_3^2}{8\pi^2} \int_0^1 dt_1 \int_0^1 \frac{dt_2}{z_3^2 (t_2 - t_1)^2 + a^2} \,. \quad (3.3)$$

Calculating the integrals gives the result

$$\Gamma_\Sigma(z_3, a) = -\, C_F \frac{\alpha_s}{2\pi} \left[2 \frac{|z_3|}{a} \tan^{-1}\left(\frac{|z_3|}{a}\right) - \ln\left(1 + \frac{z_3^2}{a^2}\right) \right] \quad (3.4)$$

coinciding with that given in Ref. [13].

If we keep z_3 fixed and take the small-a limit, we can expand

$$\Gamma_\Sigma(z_3, a)|_{a\to 0} = -\, C_F \frac{\alpha_s}{2\pi} \left[\frac{\pi |z_3|}{a} - 2 - \ln \frac{z_3^2}{a^2} + O(a^2/z_3^2) \right] \,. \quad (3.5)$$

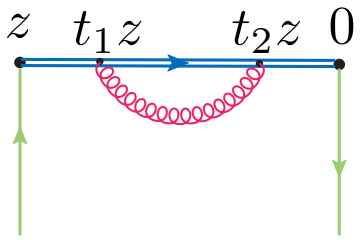

Figure 1: Renormalization of the gauge link.

This result clearly shows a linear divergence $\sim |z_3|/a$ in the $a \to 0$ limit. As explained in the pioneering paper [6], it may be interpreted as the mass renormalization δm of a test particle moving along the link,

$$\delta m = C_F \frac{\alpha_s}{2\pi} \frac{\pi}{a} \,. \quad (3.6)$$

Alternatively, for a fixed a and small z_3, the factor in the square brackets behaves like z_3^2/a^2, i.e., $\Sigma(z_3, a)$ vanishes at $z_3 = 0$. This distinctive feature of such UV contributions is a mere consequence of the fact that the gauge link converts into unity for $z_3 = 0$.

As a result, the UV terms vanish on the light cone, and that is why they are usually not discussed in the context of the light-cone PDFs. Also, the fact that $\Sigma(z_3 = 0, a) = 0$ means that, at fixed a, Σ gives no corrections to the vector current, i.e. the number of the valence quarks is not changed.

Eq. (3.5) also shows a logarithmic divergence corresponding to the anomalous dimension $2\gamma_{\rm end}$ due to two end-points of the link. In the lowest order (see, e.g. [14])

$$\gamma_{\rm end} = -\, C_F \frac{\alpha_s}{4\pi} \,. \quad (3.7)$$

In an Abelian theory, the vacuum average of an exponential is the exponential of the one-loop vacuum average. Hence, the one-loop term exponentiates. In the $a \to 0$ limit, this produces a factor

$$Z_{\rm link}(z_3, a) = e^{-\delta m |z_3|} e^{-2\gamma_{\rm end} \ln(z_3^2/a^2)} \,. \quad (3.8)$$

The exponentiation works also in a non-Abelian case [15, 16, 17], but the exponential involves then higher-α_s corrections accompanied by higher irreducible color factors. The all-order renormalization of Wilson loops and lines was discussed in Refs. [18, 19, 14].

The Polyakov prescription $1/z_3^2 \to 1/(z_3^2 + a^2)$ softens the gluonic propagator at distances $z_3 \sim$ several a, and eliminates its singularity at $z_3 = 0$. In this respect, it is similar to the UV regularization produced by a finite lattice spacing. Thus, we find it instructive to use this prescription in the studies of the UV properties of pseudo-PDFs.

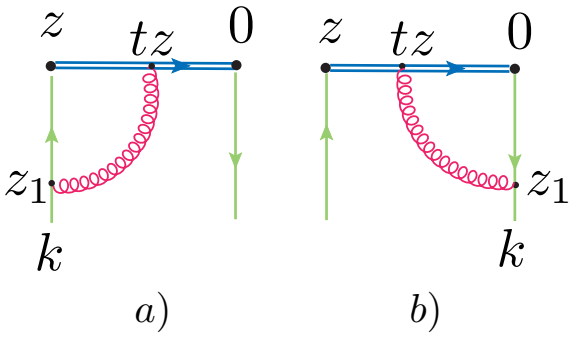

Figure 2: Insertions of gluons coming out of the gauge link.

3.2. Vertex contribution

Working in Feynman gauge, we need also to consider vertex diagrams involving gluons that connect the gauge link with the quarks, see Fig. 2.

3.2.1. Basic structure

There are two possibilities: gluon may be connected to the left (Fig. 2a) or to the right (Fig. 2b) quark leg. To facilitate integration over z_1, we write the fields at this point in the momentum representation. If the gluon is inserted into the right quark line, we start with

$$O_R^\alpha(z) = (ig)^2\, C_F \int_0^1 dt \int d^4z_1\, D^c(z_1 - tz) \times \int d^4k\, e^{i(kz_1)}\, \bar\Psi(k) \not{z} S^c(z_1) \gamma^\alpha \psi(z)] \,. \tag{3.9}$$

The insertion into the left leg gives a similar expression. Using $S^c(z) = i\not{z}/2\pi^2(z^2)^2$ and $D^c(z) = 1/4\pi^2 z^2$ combined with the representation

$$\frac{1}{(z^2/4)^{N+1}} = \frac{i^{N-1}}{N!} \int_0^\infty d\sigma \sigma^N e^{-i\sigma z^2/4} \tag{3.10}$$

gives a Gaussian integral over z_1. Taking it, we obtain

$$O_R^\alpha(z) = i\frac{g^2}{8\pi^2} C_F \int_0^1 dt \int_0^\infty \sigma_1 \frac{d\sigma_1 d\sigma_2}{(\sigma_1+\sigma_2)^3} \times \int d^4k\, e^{i(t(kz)\sigma_2 - \sigma_1\sigma_2 t^2 z^2/4)/(\sigma_1+\sigma_2)} \times \bar\Psi(k)\left[(kz) + t\sigma_2 z^2/4\right]\gamma^\alpha\psi(z) \,. \tag{3.11}$$

The external quark lines enter into the soft part, thus we neglect their virtuality, i.e. the k^2 term in the exponential. For the same reason, wee also neglect the $\bar\Psi(k)\not{k}$ term.

Switching to $\lambda_i = 1/\sigma_i$, introducing common $\lambda = \lambda_1 + \lambda_2$, with $\lambda_1/\lambda = \beta$, then relabeling $\lambda = 1/\sigma$, we obtain

$$O_R^\alpha(z) = i\,\frac{g^2}{8\pi^2} C_F \int_0^1 dt \int_0^\infty d\sigma\, e^{-i\sigma t^2 z^2/4} \int_0^1 d\beta \times \int d^4k\, e^{i\beta t(kz)}\, \bar\Psi(k)[(1-\beta)(kz)/\sigma + t\,z^2/4]\,\gamma^\alpha\psi(z) \,. \tag{3.12}$$

3.2.2. UV singular term

We can take the d^4k integral for the second, namely tz^2, term in Eq. (3.12) to get

$$O_{R2}^\alpha(z) = i\,\frac{g^2}{8\pi^2} C_F \int_0^1 dt\, t \int_0^1 d\beta \times \frac{z^2}{4}\int_0^\infty d\sigma\, e^{-i\sigma t^2 z^2/4}\, \bar\psi(t\beta z)\,\gamma^\alpha\psi(z) \,. \tag{3.13}$$

Now, integration over σ leads to an UV divergence from the small-t integration. The situation is similar to that in the case of the link renormalization. Thus, we regularize $1/z^2 \to 1/(z^2 - a^2)$ in the initial expression (3.10) for the gluon propagator. Since the singularity is accompanied by the quark field $\bar\psi(t\beta z)$ at $t = 0$, we isolate it by splitting $\bar\psi(0) + [\bar\psi(t\beta z) - \bar\psi(0)]$. The UV-singular term is then given by

$$O^\alpha_{\rm R,UV}(z,a) = \frac{g^2}{8\pi^2} C_F\, \bar\psi(0)\gamma^\alpha\psi(z) \times \int_0^1 d\beta \int_0^1 dt\, \frac{tz^2}{t^2z^2 - a^2/(1-\beta)} \,. \tag{3.14}$$

Taking integrals over t and β gives the expression

$$O^\alpha_{\rm R,UV}(z,a) = \frac{g^2}{16\pi^2} C_F\, \bar\psi(0)\gamma^\alpha\psi(z) \times \left[\left(1 - \frac{a^2}{z^2}\right)\ln\left(1 - \frac{z^2}{a^2}\right) - 1\right] \tag{3.15}$$

that contains the same $\ln\left(1 - z^2/a^2\right)$ logarithmic term as in the self-energy correction (3.4). The diagram with the insertion into the left leg gives the same contribution, thus the total UV-singular contribution doubles $O^\alpha_{\rm UV}(z,a) = 2O^\alpha_{\rm R,UV}(z,a)$.

Switching to $z = z_3$, we have the $\ln(z_3^2/a^2)$ structure in the $a \to 0$ limit, and we may combine it with the UV divergences generated by the link self-energy diagrams. Again, for a fixed a, the $O^\alpha_{\rm UV}(z_3,a)$ contribution vanishes in the $z_3^2 \to 0$ limit.

3.2.3. UV finite term

The $[\bar\psi(t\beta z) - \bar\psi(0)]$ term vanishes for $t = 0$, and for this reason its contribution

$$O^\alpha_{\rm R,reg}(z_3,a) = \frac{g^2}{8\pi^2} C_F\, z_3^2 \int_0^1 dt\, t \int_t^1 \frac{d\beta}{t^2 z_3^2 + \beta^2 a^2/(1-\beta)} \times [\bar\psi(tz_3)\gamma^\alpha\psi(z_3) - \bar\psi(0)\gamma^\alpha\psi(z_3)] \tag{3.16}$$

is finite in the $a \to 0$ limit. Taking $a = 0$ and integrating over β gives

$$O^\alpha_{\rm R,reg}(z_3, a=0) = \frac{\alpha_s}{2\pi} C_F \int_0^1 du \left[\frac{\bar u}{u}\right]_+ \bar\psi(uz_3)\gamma^\alpha\psi(z_3) \,, \tag{3.17}$$

where we have relabeled $t \to u$, and introduced $\bar u \equiv 1 - u$. The plus-prescription is defined by

$$\int_0^1 du \left[\frac{\bar u}{u}\right]_+ F(u) = \int_0^1 du\, \frac{\bar u}{u}\,[F(u) - F[0] \,, \tag{3.18}$$

assuming that $F(0)$ is finite. Again, the plus-prescription structure of Eq. (3.17) guarantees that this term gives no corrections to the local current.

Adding the contribution of the diagram with the left-leg insertion, we may write the total regular term as

$$O^{\alpha}_{\rm reg}(z_3, a=0) = \frac{\alpha_s}{2\pi}\, C_F \int_0^1 du \int_0^1 dv\, \bar\psi(uz_3)\gamma^\alpha\psi(\bar v z_3) \times \left\{\delta(v)\left[\frac{\bar u}{u}\right]_+ + \delta(u)\left[\frac{\bar v}{v}\right]_+\right\} . \quad (3.19)$$

In terminology of Balitsky and Braun [8], $\bar\psi(uz)\gamma^\alpha\psi(\bar v z)$ is a "string operator". It involves two fields on the straight line segment $(0, z)$, separated from its endpoints by uz and vz, respectively. The difference with Ref. [8] is that z here is not on the light cone $z^2 = 0$.

3.2.4. Evolution terms

Now, let us analyze the $(1-\beta)(kz)/\sigma$ term in Eq. (3.12),

$$O^{\alpha}_{\rm R,Evol}(z) = i\,\frac{g^2}{8\pi^2}\, C_F \int_0^1 dt \int_0^\infty \frac{d\sigma}{\sigma}\, e^{-i\sigma t^2 z^2/4} \int_0^1 d\beta\,(1-\beta) \times \int d^4k\,(kz)\, e^{it\beta(kz)}\bar\Psi(k)\gamma^\alpha\psi(z) . \quad (3.20)$$

This expression has a logarithmic infrared divergence resulting from the lower limit of the σ integration.

In fact, if we would keep the k^2 term in the exponential of Eq. (3.11), it would produce a $e^{ik^2/\sigma}$-type factor in the expression above, and there would be no infrared divergency. In other words, the quark virtuality would provide an IR cut-off. In the coordinate representation, this corresponds to a cut-off produced by the nonperturbative z_1^2-dependence of the soft matrix element $\langle p|\bar\psi(0)\gamma\psi(z_1)|p\rangle$ (we refer here to Fig.2 a).

An example of calculations, in which such a dependence was taken into account, may be found in our paper [9], where the virtuality distribution formalism was applied to the pion transition form factor. In our present context, the cut-off will be provided by the $k_\perp$-dependence of the soft part of the TMD $\mathcal{F}(x, k_\perp^2)$, i.e. by the hadron size. Leaving a detailed investigation for future studies, we will just assume now some reasonable form of an IR cut-off function.

In particular, the IR singularity may be regularized by the $e^{-im^2/\sigma}$ factor, which is equivalent to adding the same mass term m^2 to both propagators. In this case (switching to $z^2 = -z_3^2$), we define

$$L_m(t^2 z_3^2 m^2) \equiv \int_0^\infty \frac{d\sigma}{\sigma}\, e^{i\sigma t^2 z_3^2/4 - im^2/\sigma} = 2K_0(tm|z_3|) . \quad (3.21)$$

This function has a logarithmic $\ln z_3^2 m^2$ singularity for small z_3 and an exponential $e^{-|z_3|m}$ fall-off for large z_3. One should realize that since m parametrizes the IR cut-off imposed by the hadron size, numerically m should be of an order of 0.5 GeV.

Another simple possibility to regularize the IR singularity is to cut the σ-integral from below. Then we have

$$L_{1/z_0}(t^2 z_3^2/z_0^2) \equiv \int_{1/z_0^2}^\infty \frac{d\sigma}{\sigma}\, e^{i\sigma t^2 z_3^2/4} = \Gamma[0, t^2 z_3^2/4z_0^2] , \quad (3.22)$$

where $\Gamma[0, x]$ is the incomplete gamma-function. Again, we have a logarithmic $\ln z_3^2/z_0^2$ singularity for small z_3, but now a Gaussian $e^{-z_3^2/4z_0^2}$ behavior for large z_3. As observed in Ref. [9], the two forms of the IR cut-off automatically follow from soft distributions with exponential and Gaussian fall-off at large $z_\perp$, respectively.

For small $|z_3|$, we may write in both cases

$$L_\Lambda(t^2 z_3^2\Lambda^2) = L_\Lambda(z_3^2\Lambda^2) - 2\ln t + O(\Lambda^2 z_3^2) . \quad (3.23)$$

The logarithms $\ln(z_3^2\Lambda^2)$ contained in $L_R(z_3^2\Lambda^2)$ reflect the perturbative evolution.

Integrating over t in the part corresponding to the $L_\Lambda(z_3^2\Lambda^2)$ term in Eq. (3.23), changing the notation $\beta \to v$, and adding the contribution from the left-leg insertion, we get the total logarithmic contribution

$$O^{\alpha}_{\rm log}(z_3) = L_\Lambda(z_3^2\Lambda^2)\,\frac{\alpha_s}{2\pi}\, C_F \int_0^1 du \int_0^1 dv \times \left\{\delta(u)\left[\frac{\bar v}{v}\right]_+ + \delta(v)\left[\frac{\bar u}{u}\right]_+\right\} \bar\psi(uz_3)\gamma^\alpha\psi(\bar v z_3) . \quad (3.24)$$

For small z_3^2, this result corresponds to the following correction to the ITD

$$\mathcal{M}_{\rm log}(\nu, z_3^2) = L_\Lambda(z_3^2\Lambda^2)\,\frac{\alpha_s}{2\pi}\, C_F \int_0^1 dw \left[\frac{2w}{1-w}\right]_+ \mathcal{M}^{\rm soft}(w\nu, 0) . \quad (3.25)$$

Note that, in contrast to the UV divergent contribution, the $L_\Lambda(z_3^2\Lambda^2)$ function is singular in the $z_3^2 \to 0$ limit, and $|z_3|$ in the integrals of Eqs. (3.21), (3.22) works like an ultraviolet rather than an infra-red cut-off.

3.2.5. IR finite term

The $\ln t$-term in Eq. (3.23) produces an IR finite contribution

$$O^{\alpha}_{\rm R,Fin}(z) = -\,i\,\frac{g^2}{4\pi^2}\, C_F \int_0^1 dt\, \ln t \int_0^1 d\beta\,(1-\beta) \times \int d^4k\,(kz)\, e^{it\beta(kz)}\,\bar\Psi(k)\gamma^\alpha\psi(z) . \quad (3.26)$$

Transforming the β-integral through integrating exponential by parts, changing $\beta = v/t$ and adding the left $O^{\alpha}_{\rm L,Fin}(z)$ contribution, we obtain

$$O^{\alpha}_{\rm Fin}(z) = -\,\frac{\alpha_s}{\pi}\, C_F \int_0^1 du \int_0^1 dv\, \bar\psi(vz)\gamma^\alpha\psi(\bar u z) \times [\delta(u)\, s_+(v) + \delta(v)\, s_+(u)] , \quad (3.27)$$

where $s_+(u)$ is the plus-prescripted version of $s(u)$ given by

$$s(u) \equiv \int_u^1 dt\,\frac{\ln t}{t^2} = \frac{1-u+\log(u)}{u} . \quad (3.28)$$

Since this part depends on z through the fields only, we deal with a finite radiative correction to the soft contribution.

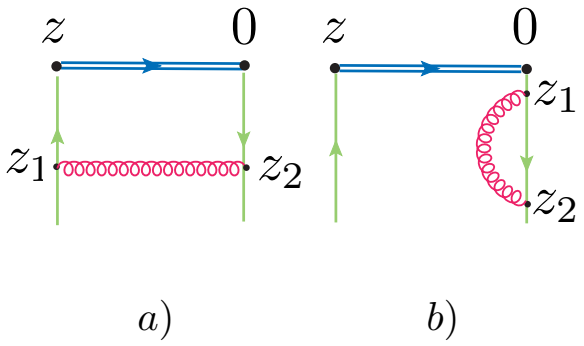

Figure 3: a) Gluon exchange diagram. b) One of quark self-energy correction diagrams.

3.3. Quark-gluon exchange contribution

There is also a contribution to the hard part given by the diagram 3a containing a gluon exchange between two quark lines. Taking the time component $\alpha = 0$, we have

$$O^0_{\rm exch}(z_3) = \frac{\alpha_s}{2\pi} C_F \int_0^1 du \int_0^{1-u} dv \times \left\{L_R(z_3^2R^2) + 1\right\} \bar\psi(uz_3)\gamma^\alpha\psi(\bar v z_3)\,. \quad (3.29)$$

For the ITD, this gives the integral

$$\mathcal{M}_{\rm exch}(\nu, z_3^2) = \frac{\alpha_s}{2\pi} C_F \int_0^1 dw\,(1-w) \times \left\{L_R(z_3^2R^2) + 1\right\} \mathcal{M}^{\rm soft}(w\nu, 0) \quad (3.30)$$

with the $(1-w)$ integrand. Its logarithmic part, combined with the $2w/(1-w)$ term coming from the vertex correction, gives the expected form $(1+w^2)/(1-w)$ of the evolution kernel. Note, however, that unlike the vertex part, the exchange contribution (3.30) does not have the plus-prescription form.

The standard expectation is that one would get it after the addition of the quark self-energy diagrams, one of which is shown in Fig. 3b. As usual, one should take just a half of each, absorbing the other halves into the soft part. These diagrams have an ultraviolet divergence that may be regularized by the same (for uniformity) Polyakov prescription $1/z^2 \to 1/(z^2 - a^2)$ for the gluon propagator. The result is a $\ln(a^2m^2)$ contribution. But, since it has no z-dependence, it cannot help one to get the plus-prescription form for the logarithmic part of the exchange contribution.

A possible way out is to represent $\ln(a^2m^2)$ as the difference $\ln(z_3^2m^2) - \ln(z_3^2/a^2)$ of the evolution-type logarithm $\ln(z_3^2m^2)$ and a UV-type logarithm $\ln(z_3^2/a^2)$. The latter can be added to the UV divergences of the diagrams 1 and 2, so that the total UV divergent contribution is

$$\Gamma_{\rm UV}(z_3, a) = -\frac{\alpha_s}{2\pi} C_F \left[2\frac{|z_3|}{a} \tan^{-1}\left(\frac{|z_3|}{a}\right) - 2\ln\left(1 + \frac{z_3^2}{a^2}\right) + \frac{1}{2}\ln\left(\frac{z_3^2}{a^2}\right)\right]. \quad (3.31)$$

The $\ln(z_3^2m^2)$ part should be added to the evolution kernel, and it converts the $(1-w)$ term into $(1-w)_+$.

3.4. Reduced Ioffe-time distribution

Another possibility is to use the reduced Ioffe-time distribution of Refs. [2, 20]

$$\mathfrak{M}(\nu, z_3^2) \equiv \frac{\mathcal{M}(\nu, z_3^2)}{\mathcal{M}(0, z_3^2)}\,. \quad (3.32)$$

Then the UV divergences generated by the link-related and quark-self-energy diagrams cancel in the ratio (3.32). Furthermore, since $\nu = 0$ is equivalent to $p = 0$, the denominator factor automatically completes the gluon-exchange contribution $(1-w)$ to $(1-w)_+$.

The vertex part (3.25) of the evolution kernel has the plus-prescription structure from the start. For this reason, it does not contribute to the denominator factor $\mathcal{M}(0, z_3^2)$. As a result, $\mathfrak{M}(\nu, z_3^2)$ satisfies the evolution equation

$$\frac{d}{d\ln z_3^2}\mathfrak{M}(\nu, z_3^2) = -\frac{\alpha_s}{2\pi} C_F \int_0^1 dw\, B(w)\mathfrak{M}(w\nu, z_3^2) \quad (3.33)$$

with respect to z_3^2, where $B(w)$ is the full plus-prescription Altarelli-Parisi (AP) evolution kernel [21]

$$B(w) = \left[\frac{1+w^2}{1-w}\right]_+\,. \quad (3.34)$$

There are also non-logarithmic terms[1] from (3.19) and (3.27) that contribute to the numerator factor ITD $\mathcal{M}(\nu, z_3^2)$. However, since they have the plus-prescription structure, they vanish in the denominator factor $\mathcal{M}(0, z_3^2)$. Thus, we get the one-loop expression for the hard part of the reduced ITD in the following form

$$\mathfrak{M}^{\rm hard}(\nu, z_3^2) = -\frac{\alpha_s}{2\pi} C_F \int_0^1 dw \left\{\left(\frac{1+w^2}{1-w}\right)_+ \left[\ln(z_3^2m^2e^{2\gamma_E}/4) + 1\right] + 4\left(\frac{w + \log(1-w)}{1-w}\right)_+\right\} \mathfrak{M}^{\rm soft}(w\nu, 0)\,, \quad (3.35)$$

where we also have explicitly displayed the logarithmic part of the modified Bessel function $K_0(|z_3|m)$.

4. Hard contribution to quasi-PDFs

The Ioffe-time distributions are basic starting objects for all parton distributions. Hence, the results obtained above may be used to calculate the one-loop corrections for quasi-PDFs. In what follows, we analyze how the z_3^2-dependence of $\mathcal{M}_{\rm UV}(\nu, z_3^2)$ is reflected in some specific features of quasi-PDFs.

[1] Such terms also appear in the expression for the pseudo-PDF in Ref. [22], but there is a discrepancy with our results.

4.1. Ultraviolet divergent terms

For the UV-singular terms, we have

$$\mathcal{M}_{\rm UV}(\nu, z_3^2) = \Gamma_{\rm UV}(z_3, a)\, \mathcal{M}^{\rm soft}(\nu, 0)\,. \tag{4.1}$$

Combining the definition (2.6) of the quasi-PDFs with the relation (2.4) between $\mathfrak{M}(\nu, 0)$ and the PDF $f(x)$ we have

$$Q_{\rm UV}(y, P) = \int_{-1}^{1} dx\, R_{\rm UV}(y - x; a)\, f(x)\,, \tag{4.2}$$

where

$$R_{\rm UV}(y - x; a) = \frac{P}{2\pi} \int_{-\infty}^{\infty} dz_3\, e^{-i(y-x)Pz_3}\, \Gamma_{\rm UV}(z_3, a)\,. \tag{4.3}$$

For the link renormalization correction Γ_Σ, this Fourier transform can be easily done using its original representation (3.3), producing

$$R_\Sigma(y, x; Pa) = \frac{\alpha_s}{2\pi}\, \frac{1}{Pa} \left[\frac{e^{-|y-x|Pa}}{(y-x)^2} - \delta(y-x) \int_{-\infty}^{\infty} \frac{d\zeta}{(\zeta - x)^2} e^{-|\zeta - x|Pa} \right]. \tag{4.4}$$

Note that, due to the exponential suppression factor, the ζ-integral accompanying the $\delta(y - x)$ term converges when $\zeta \to \pm\infty$. As a result, $R_\Sigma(y, x; Pa)$ is given by a mathematically well-defined expression.

The $1/Pa$ term in Eq. (4.4) corresponds to the linear UV divergence. Expanding $e^{-|y-x|Pa}$ in a gives the $1/|y - x|$ term corresponding to the logarithmic $\ln(1 + z_3^2/a^2)$ UV divergence in Eq. (3.4). As we have seen, the same $\ln(1 + z_3^2/a^2)$ UV contribution appears in the vertex corrections. Calculating the Fourier transform of $\ln(1 + z_3^2/a^2)$ gives

$$R_V(y, x; Pa) = -\frac{\alpha_s}{2\pi} \left[\frac{1}{|y-x|} e^{-|y-x|Pa} - \delta(y-x) \int_{-\infty}^{\infty} \frac{d\zeta}{|y-\zeta|} e^{-|y-\zeta|Pa} \right]. \tag{4.5}$$

Now we can represent $R_\Sigma(y, x; Pa)$ as a sum

$$R_\Sigma(y, x; Pa) = \frac{\alpha_s}{2\pi} \left[e^{-|y-x|Pa} \left(\frac{1}{Pa(y-x)^2} + \frac{1}{|y-x|} \right) - \delta(y-x) \int_{-\infty}^{\infty} d\zeta\, e^{-|\zeta-x|Pa} \left(\frac{1}{Pa(\zeta-x)^2} + \frac{1}{|\zeta-x|} \right) \right] + R_V(y, x; Pa)\,. \tag{4.6}$$

of the regularized $1/(y-x)^2$ singularity corresponding to the linear divergence and the vertex kernel $R_V(y, x; Pa)$ corresponding to the logarithmic divergence.

4.2. Evolution-related terms

Let us consider now the hard part given by the evolution logarithms

$$\mathcal{M}_{\log}(\nu, z_3^2) = -\frac{\alpha_s}{2\pi}\, C_F\, L_\Lambda(z_3^2\Lambda^2) \int_0^1 du\, B(u)\, \mathcal{M}^{\rm soft}(u\nu, 0)\,. \tag{4.7}$$

In this case

$$Q_{\log}(y, P) = C_F\, \frac{\alpha_s}{2\pi} \int_{-1}^{1} d\xi\; f(\xi) \int_0^1 du\, B(u)\, K(y - u\xi; \Lambda^2/P^2)\,, \tag{4.8}$$

where the kernel $K(y - u\xi; \Lambda^2/P^2)$ is given by the Fourier transform of $L_\Lambda(z_3^2\Lambda^2)$. If we choose the IR regularization of Eq. (3.21) leading to the modified Bessel function $K_0(mz_3)$, we have

$$K(y - x, m^2/P^2) = \frac{P}{2\pi} \int_{-\infty}^{\infty} dz_3\, e^{-i(y-x)Pz_3}\, K_0(m|z_3|) = \frac{1}{\sqrt{(y-x)^2 + m^2/P^2}}\,. \tag{4.9}$$

We may also write

$$Q_{\log}(y, P) = C_F\, \frac{\alpha_s}{2\pi} \int_{-1}^{1} \frac{d\xi}{|\xi|} R(y/\xi, m^2/\xi^2P^2)\, f(\xi)\,, \tag{4.10}$$

where the kernel $R(\eta, m^2/P^2)$ is given by

$$R(\eta; m^2/P^2) = \int_0^1 \frac{du}{\sqrt{(\eta - u)^2 + m^2/P^2}} \left[\frac{1 + u^2}{1 - u} \right]_+. \tag{4.11}$$

It is convenient to consider the cases $\xi > 0$ and $\xi < 0$ separately. Let us take $\xi > 0$ which corresponds to $f(\xi)$ being nonzero for positive ξ only.

Simply taking $m^2/P^2 = 0$ results in a factor $1/|\eta - u|$ containing a non-integrable singularity for $u = \eta$. With respect to integration over the $0 \le u \le 1$ interval, we may display it as

$$\left. \frac{1}{\sqrt{(\eta - u)^2 + m^2/P^2}} \right|_{m^2/P^2 \to 0} = \left(\frac{1}{|\eta - u|} \right)_+ + \delta(\eta - u) \ln \left[4\eta(1 - \eta) \frac{P^2}{m^2} \right] \theta[0 \le \eta \le 1]\,, \tag{4.12}$$

where the plus-prescription is defined by

$$\left(\frac{1}{|\eta - u|} \right)_+ = \frac{1}{|\eta - u|} - \delta(\eta - u) \int_0^1 \frac{dv}{|\eta - v|}\,. \tag{4.13}$$

4.2.1. Middle part

From the $\delta(\eta - u)$ part we get the evolution term

$$R_1^{\rm middle}(\eta; m^2/P^2) = \ln\left(\frac{4P^2}{m^2} \right) \left[\frac{1 + \eta^2}{1 - \eta} \theta(0 \le \eta \le 1) \right]_+, \tag{4.14}$$

that is present in the $0 \le \eta \le 1$ region only. The terms coming from $(1/|\eta - u|)_+$ are given in this region by

$$R_2^{\rm middle}(\eta) = \frac{1 + \eta^2}{1 - \eta} \log\left[\eta(1 - \eta) \right] + \frac{3/2}{1 - \eta} + 4\frac{\log(1 - \eta)}{1 - \eta} - 1 + 2\eta\,. \tag{4.15}$$

4.2.2. Outer parts

For η outside the $0 \le \eta \le 1$ segment, the $m^2/P^2 \to 0$ limit is finite and given by

$$R(\eta;0)|_{\eta>1} = \int_0^1 \frac{du}{\eta-u}\left[\frac{1+u^2}{1-u}\right]_+ = -\sum_{n=1}^{\infty}\frac{\gamma_n}{\eta^{n+1}}\,, \qquad (4.16)$$

where γ_n are the anomalous dimensions of operators with n derivatives

$$\gamma_n = \int_0^1 du\,\frac{1-u^n}{1-u}(1+u^2) = 2\sum_{j=1}^{n+1}\frac{1}{j} - \frac{3}{2} - \frac{1}{(n+1)(n+2)}\,. \qquad (4.17)$$

At first sight, one would expect a $\sim 1/|\eta|$ behavior for large $|\eta|$. However, the $1/|\eta|$ term is accompanied by the integral of $P(u)$ which vanishes because of the plus-prescription. This is also the reason why γ_0 vanishes causing the series in Eq. (4.16) to start at $n = 1$. In a closed form,[2]

$$R(\eta;0)|_{\eta>1} = \frac{1+\eta^2}{\eta-1}\ln\left(\frac{\eta-1}{\eta}\right) + \frac{3}{2(\eta-1)} + 1\,. \qquad (4.18)$$

Similarly, for $\eta < 0$

$$R(\eta;0)|_{\eta<0} = \frac{1+\eta^2}{1-\eta}\ln\left(\frac{1-\eta}{-\eta}\right) + \frac{3}{2(1-\eta)} - 1\,. \qquad (4.19)$$

One may notice here the $\pm\frac{3}{2}/(1-\eta)$ terms having the evident $\sim 1/|\eta|$ behavior. But these terms exactly cancel the $\sim 1/|\eta|$ contributions coming from the remaining terms, thus changing the large-η behavior to $\sim 1/\eta^2$. We have already seen the $\sim -1/\eta^2$ asymptotic behavior for $\eta > 1$ in Eq.(4.16). Similarly, for large negative values, one may use the expansion

$$R(\eta;0)|_{\eta<-1} = \sum_{n=1}^{\infty}\frac{\gamma_n}{\eta^{n+1}}\,. \qquad (4.20)$$

Thus, for large $|\eta|$ we have the asymptotic behavior

$$R(\eta;0)|_{|\eta|\gg 1} = -\frac{4}{3}\frac{\mathrm{sgn}(\eta)}{\eta^2} + O(1/\eta^3)\,. \qquad (4.21)$$

4.3. Plus-prescription

The $\sim 1/y^2$ result for $R(y/\xi;m^2/P^2)$ may be foreseen if one notices that calculating it from the convolution with the AP kernel (see Eq. (4.11)), one deals with the difference

$$\frac{1}{\sqrt{(y-u\xi)^2+m^2/P^2}} - \frac{1}{\sqrt{(y-\xi)^2+m^2/P^2}}\,, \qquad (4.22)$$

which behaves like $1/y^2$ for large y. Hence, the integral of $R(y/\xi;m^2/P^2)$ over y does not have divergences for large $|y|$.

[2]Comparing our results with those of Ref. [23], one should take into account that the evolution-related contributions are combined there with the UV-singular terms taken in the limit equivalent to our $a \to 0$.

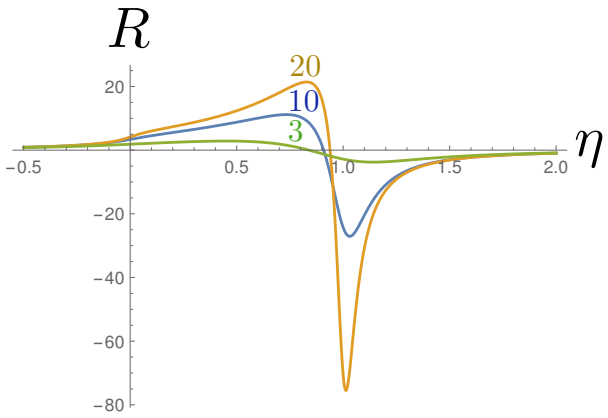

Figure 4: The kernel $R(\eta, m^2/P^2)$ for $P/m = 3$, 10 and 20.

Moreover, since the two terms differ just by a shift in the y-variable, the integral vanishes. As a result, we have

$$\int_{-\infty}^{\infty} dy\, R(y/\xi;m^2/P^2) = 0\,, \qquad (4.23)$$

which leads to

$$\int_{-\infty}^{\infty} dy\, Q_{\log}(y,P) = 0\,, \qquad (4.24)$$

i.e. the evolution part does not change the quark number.

4.4. R-kernel at finite momenta

Results for $R(\eta)$ correspond to the full function $R(\eta, m^2/P^2)$ taken in the $P^2/m^2 \to \infty$ limit. However, since m should be understood as an IR cut-off provided by the hadron size, it has a rather large ~ 0.5 GeV magnitude. On the other hand, the maximal momenta P reached in actual lattice calculations of the quasi-PDFs [24, 25] range from 1.3 to about 2.5 GeV. Thus, it is interesting to look at the P/m-dependence of $R(\eta, m^2/P^2)$.

In Fig. 4, we show the structure of the kernel $R(\eta;m^2/P^2)$ for three values of P/m. In the central segment $0 < \eta < 1$, it has the evolution part (4.14) proportional to $\ln(P^2/m^2)$. This term is the main reason for the increase of R with P in this region. A large negative peak in the $y \sim 1$ region also increases its magnitude as $\ln(P^2/m^2)$. It reflects the $\delta(1-\eta)$ plus-prescription term in the AP kernel.

Note that since the evolution part (4.14) has the plus-prescription form, its contribution to the integral (4.23) is zero. There are, in addition, non-logarithmic parts (4.15), (4.18), (4.19), and their combined contribution to the integral (4.23) should also vanish. This means that in the $P/m \to \infty$ limit the negative peak for $\eta = 1$ should contain also a non-logarithmic (in P^2/m^2) part that provides plus-prescription for each of these contributions. For instance, when $\eta > 1$, we would have

$$R(\eta;0)|_{\eta>1} \to R(\eta;0)|_{\eta>1} - \delta(\eta-1)\int_1^{\infty} d\zeta R(\zeta;0)\,. \qquad (4.25)$$

The integral over ζ here diverges when $\zeta \to 1$, but this is what is expected from the plus-prescription construction. For $\zeta \to \infty$,

the integral converges, hence Eq. (4.25) is a mathematically well-defined expression. For nonzero m/P, we should have, of course, some smoothened version of $\delta(1-\eta)$.

Looking at the curve corresponding to $P/m = 3$ (the value, realistically corresponding to the momentum $P \sim 1.5$ GeV), one can see that "smoothened" in this case is a strong understatement. This curve does not show anything resembling a delta-function near $\eta = 1$. The reason for a big difference between the finite-P curves and their $P \to \infty$ limit may be traced to the basic relation (2.6) between quasi-PDFs and pseudo-PDFs: the y-shape of quasi-PDFs $Q(y, P)$ is strongly distorted by the large-z_3 nonperturbative behavior of the pseudo-PDFs $\mathcal{P}(x, z_3^2)$. One needs large momenta P (and some deconvolution techniques) just to get rid of this contaminating large-z_3 information.

In contrast, if one does not like to use large z_3 values working with the pseudo-PDFs, one can simply exclude them from the analysis. Moreover, since the impact parameter distribution $\mathcal{P}(x, z_\perp^2)$ of the TMD studies has the same functional form as the pseudo-PDF $\mathcal{P}(x, z_3^2)$, one can use the large-z_3 data to get a direct information about the 3-dimensional hadron structure.

5. Summary.

In this paper, we have studied the small-z_3^2 behavior of the Ioffe-time distribution $\mathcal{M}(\nu, z_3^2)$ at one-loop level. The ITD is the basic function that may be converted, in a prescribed way, into pseudo-PDFs and quasi-PDFs. In its turn, the short-distance structure of the ITD is determined by that of the underlying bilocal operator $O^\alpha(0, z) = \bar\psi(0)\gamma^\alpha E(0, z; A)\psi(z)$. Since the corrections to $O^\alpha(0, z)$ may be calculated on the operator level, it is an even more fundamental object.

In our study, we made an effort to separate two sources of the z_3^2-dependence at small z_3^2. One is related to the UV singularities generated by the gauge link $E(0, z_3; A)$ connecting the quark fields forming the QCD bilocal operator. The logarithmic part of these terms has the $\ln(1 + z_3^2/a^2)$ structure, where a is the UV cut-off parameter analogous to lattice spacing. Thus, while being singular in the $a \to 0$ limit, the $\ln(1 + z_3^2/a^2)$ factor vanishes for $z_3^2 = 0$. This is a general property of the link-related UV-singular terms. It is a very important one since it guarantees that such corrections do not change the number of valence quarks.

The one-loop UV divergencies are eliminated if one considers the reduced ITD $\mathfrak{M}(\nu, z_3^2)$ given by the ratio $\mathcal{M}(\nu, z_3^2)/\mathcal{M}(0, z_3^2)$. Still, $\mathfrak{M}(\nu, z_3^2)$ has a non-trivial short-distance behavior. At one loop, it has the $\ln z_3^2\Lambda^2$ structure, where Λ is an IR cut-off parameter. These terms generate perturbative evolution of the parton densities. While they are singular in the $z_3^2 \to 0$ limit, the evolution corrections do not change the number of valence quarks. This is secured by the fact that the ν-dependence of such corrections is governed by factors possessing the plus-prescription property. The explicit expression that we give for the z_3^2-dependence of the reduced ITD at one loop, may (and will) be used in our future work on extraction of PDFs from the lattice QCD simulations using the pseudo-PDF-based methodology.

We have also demonstrated that our results may be used for a rather straightforward calculation of the one-loop corrections to quasi-PDFs, providing new insights concerning their structure.

As emphasized above, the corrections to the bilocal operator $O^\alpha(0, z)$ may be calculated without specifying a matrix element in which it is embedded. In particular, changing the $\langle p|...|p\rangle$ brackets into $\langle 0|...|p\rangle$, one may use the results of the present paper to get one-loop corrections to pseudo- and quasi-distribution amplitudes. Similarly, taking the $\langle p_1|...|p_2\rangle$ matrix elements, one can get one-loop results for generalized parton pseudo-distributions ("pseudo-GPDs"). These are natural directions for future studies.

Acknowledgements. I thank I. Balitsky, V.M. Braun and J.-W. Qiu for discussions and K. Orginos and for his interest in this work. This work is supported by Jefferson Science Associates, LLC under U.S. DOE Contract #DE-AC05-06OR23177 and by U.S. DOE Grant #DE-FG02-97ER41028.

[1] R. P. Feynman, Phys. Rev. Lett. **23** (1969) 1415.
[2] A. V. Radyushkin, Phys. Rev. D **96** (2017) no.3, 034025
[3] B. L. Ioffe, Phys. Lett. **30B** (1969) 123.
[4] X. Ji, Phys. Rev. Lett. **110** (2013) 262002
[5] V. Braun, P. Gornicki and L. Mankiewicz, Phys. Rev. D **51** (1995) 6036
[6] A. M. Polyakov, Nucl. Phys. B **164** (1980) 171.
[7] N. S. Craigie and H. Dorn, Nucl. Phys. B **185** (1981) 204.
[8] I. I. Balitsky and V. M. Braun, Nucl. Phys. B **311** (1989) 541.
[9] A. V. Radyushkin, Phys. Rev. D **93** (2016) no.5, 056002
[10] A. V. Radyushkin, Phys. Lett. B **735** (2014) 417
[11] A. Radyushkin, Phys. Lett. B **767** (2017) 314
[12] A. V. Radyushkin, Phys. Lett. **131B** (1983) 179.
[13] J. W. Chen, X. Ji and J. H. Zhang, Nucl. Phys. B **915** (2017) 1
[14] S. Aoyama, Nucl. Phys. B **194** (1982) 513.
[15] J. G. M. Gatheral, Phys. Lett. **133B** (1983) 90.
[16] J. Frenkel and J. C. Taylor, Nucl. Phys. B **246** (1984) 231.
[17] G. P. Korchemsky and A. V. Radyushkin, Nucl. Phys. B **283** (1987) 342.
[18] V. S. Dotsenko and S. N. Vergeles, Nucl. Phys. B **169** (1980) 527.
[19] R. A. Brandt, F. Neri and M. a. Sato, Phys. Rev. D **24** (1981) 879.
[20] K. Orginos, A. Radyushkin, J. Karpie and S. Zafeiropoulos, arXiv:1706.05373 [hep-ph].
[21] G. Altarelli and G. Parisi, Nucl. Phys. B **126** (1977) 298.
[22] X. Ji, J. H. Zhang and Y. Zhao, Nucl. Phys. B **924** (2017) 366
[23] X. Ji and J. H. Zhang, Phys. Rev. D **92** (2015) 034006
[24] H. W. Lin, J. W. Chen, S. D. Cohen and X. Ji, Phys. Rev. D **91** (2015) 054510
[25] C. Alexandrou, K. Cichy, M. Constantinou, K. Hadjiyiannakou, K. Jansen, F. Steffens and C. Wiese, Phys. Rev. D **96** (2017) no.1, 014513